Int. J. Electrochem. Sci., 11 **(2016)** 2650 - 2658

International Journal of ELECTROCHEMICAL SCIENCE
www.electrochemsci.org

Amperometric Determination of Nicotine using a Composite of Palladium hexacyanoferrate incorporated Graphene oxide modified Electrode

Cheng Yu Yang, Min-Hui Chang, Shen-Ming Chen, Balamurugan Devadas*

Electroanalysis and Bio electrochemistry Laboratory, Department of Chemical Engineering and Biotechnology, National Taipei University of Technology, No.1, Section 3, Chung-Hsiao East Road, Taipei 106, Taiwan (ROC)
*E-mail: smchen78@ms15.hinet.net

Received: 22 December 2015 / *Accepted:* 6 February 2016 / *Published:* 1 March 2016

Herein, we report a highly sensitive amperometric nicotine (NIC) sensor using composite of palladium hexacyanoferrate (PdHCF) with graphene oxide (GO) modified glassy carbon electrode (GCE). The PdHCF particles were deposited on GO modified GCE using an electrochemical method. The electrocatalytic measurements and surface morphology of the as prepared composite modified electrode were studied using cyclic voltammetry, amperometry, electrochemical impedance spectroscopy and scanning electron microscopy. The PdHCF incorporated GO composite modified electrode exhibits a prominent electrocatalytic activity towards the NIC than that of other modified electrodes. Furthermore, the presence of GO with PdHCF has greatly enhanced the surface coverage concentration and electron transfer rate constant when compared to only PdHCF and GO. The composite modified electrode shows the linear range from 8 to 240 μM for NIC with the analytical sensitivity of 1.208 μA $\mu M^{-1} cm^{-2}$.

Keywords: Palladium hexacyanoferrate, graphene oxide, nicotine, amperometry, electrochemical method.

1. INTRODUCTION

Nicotine (NIC) is the potentially active alkaloid compound containing 3^{o} amine structure of pyridine and pyrrolidine ring present in the tobacco leaves. The NIC has also been widely used as an insecticide in the field of crop production [1, 2]. The most primary reason for ingestion of NT to the human body is because of smoking; Hence, depressed smokers carrying several disorders such as co-occurring, suicide attempts, physical problem, inability to work etc. [3]. Moreover, NIC causes many problems in human body including the heart rate acceleration, blood pressure, coronary and peripheral vascular disease, hypertension, delayed wound healing, perinatal disorders, oesophageal reflux, and cancer of different organs [4, 5]. Nonetheless the NIC is widely utilized as drug, chronic nicotine involves in therapeutic of pancreatic cancer [6]. Therefore, it's significant to the detection of NIC for human health, environment necessity, medicine, toxicology and tobacco industries. So far, several analytical methods have been used for NIC analysis such as surface enhanced Raman spectroscopy (SERS) [7], photoacoustic spectroscopy (PA) [8], HPLC-UV method [9], gas chromatographic-mass spectrometric method (GC/MS) [10, 11]. Electrochemical methods are recently employed for the determination of NIC. Compared with other available methods, electrochemical methods are more reliable, cheap, sensitive and easy to operate.

Recently, different modified electrodes have been used for the determination of NIC, such as boron doped diamond (BDD) [12, 13], pencil graphite [14], activated glassy carbon electrode (GCE) [15]. On the other hand, metal hexacyanoferrate (MHCF) is a mixed valance compounds of alkali metal cation and transition metal ion [16]. Prussian blue modified electrode prepared by Neff et al., is the origin for the development of MHCF modified to many applications [17]. So far, MHCF has been widely using for several applications such as sodium and potassium ion batteries [18–20], super capacitor electrodes [21], solar cells [22], photocatalysis [23], and electrochemical sensor and biosensors [24– 27]. Among different MHCF, the palladium hexacyanoferrate (PdHCF) has also been used for the application to electrochemical sensors [28, 29]. Owing to excellent catalytic properties, higher abundance and low cost, Pd metal has been widely used for the sensor applications. On the other hand, graphene oxide (GO) is the oxidative derivative of graphite. Besides, oxygen functional moieties of GO avenues to the sensor applications [30–34]. Hence GO could be an excellent matrix material to anchor the PdHCF [35, 36]. Moreover, the composite of graphene oxide (GO) with MHCF modified electrodes have grateful attention in the field of biosensor application [37–39]. To the best of our knowledge, first time we prepare a novel composite of GO/PdHCF modified electrode for the NIC sensor application.

In this present study, the electrochemical deposition of PdHCF on GO modified GCE has been reported and used for amperometric determination of NIC. The fabricated composite modified electrode showed an excellent electrocatalytic activity towards NIC. The GO/PdHCF composite modified electrode exhibits excellent selectivity and sensitivity towards NIC.

2. EXPERIMENTAL

2.1 Materials and methods

(-)-Nicotine liquid was purchased from Sigma Aldrich. Potassium ferricyanide $K_3Fe(CN)_6$ and palladium chloride ($PdCl_2$) were obtained from Sigma Aldrich. Phosphate buffer solution (PBS) as supporting electrolyte was prepared by using sodium hydrogen phosphate and disodium hydrogen phosphate and the pH adjusted using either HCl or NaOH. All the reagents were analytical grade and used as received. All the solution was deoxygenated by purging N_2 gas for 15 minutes.

All electrochemical studies were carried out using CHI 1205A work station with three electrode system. The electrochemical cell containing working electrode (GCE with working area of 0.079 cm^2), reference electrode (Ag|AgCl in saturated KCl) and counter electrode (Pt wire). Amperometric measurements were performed with rotating ring disk electrode (RRDE-3A), BAS instrument made in Japan. Morphological studies were carried out using Hitachi S-3000 H scanning electron microscope (SEM). Energy dispersive X-ray (EDX) spectra was recorded with HORIBA EMAX X-ACT.

2.2 Synthesis of GO

Brief procedure of GO synthesis as follows. First, the commercial graphene was heated in an oven at 350^{o} C for one hour. Then the pre-heated graphene was washed with HCl (12M) and dried at room temperature. The obtained graphene was sonication in milli pure water for 4 h. Then the obtained dispersion was filtered and repeated this sonication until when the pH became neutral. The acid treated graphene was dried in oven at 100 $^{\circ}$C. Then it was re-dispersed in the acid solution containing sulphuric acid and nitric acid (3:1) and followed by ultra-sonication for 6 h. Finally, the graphene was transformed into the GO. The GO aqueous dispersion was prepared by dispersing of 1mg/mL of GO into the water with the help of sonication.

2.3 Fabrication of GO/PdHCF modified electrode

Prior to the fabrication of GO/PdHCF, the GCE was well cleaned with alumina powder followed by ultrasonication in ethanol and distilled water. About 5 µL of GO solution was pipetted out on GCE surface and dried. Then the PdHCF was electrodeposited on GO modified GCE using cyclic voltammetry (CV). Beforehand, GO modified electrode was stabilized with 10 mM of $K_3Fe(CN)_6$ solution by cyclic voltammetric (CV) scan of one cycle between the range of 1.0 to -0.4 V. Then 1 mM of $PdCl_2$ dissolved in 0.1 M H_2SO_4, was added to the ferricyanide solution. Nitrogen gas was purged through this mixture about 15 min. The stabilized GO/GCE was immersed in this solution mixture, followed by consecutive potential cycle of 20 CV scans was performed in the above mentioned range at scan rate of 50 mV/s. The detailed PdHCF deposition process are found in section 3.1. Then the PdHCF/GO modified GCE was dried at room temperature and used for electrocatalytic studies.

3. RESULTS AND DISCUSSION

3.1 Electrodeposition of PdHCF on GO modified electrode and surface characterization

The CV electrodeposition of PdHCF on GO/GCE at scan rate of 50 mV/s is expressed in Fig. 1. As shown in Fig. 1A, the redox peaks are appeared at 0.6 and 0.65 V, which corresponds to the typical process of electrochemical growth of PdHCF on GO surface. The negative scan (reduction) cycles increased linearly due to increasing the number of cycles. This growing of negative potential scale attributed to the reduction reaction of ferricyanide solution $Fe(CN)_6^{3-}$ to $Fe(CN)_6^{4-}$ [40]. The typical redox peak increases linearly which indicates the growing of PdHCF on GO modified GCE. Here, GO with negatively charged functional groups as a secondary material that allows effectively attract the positively charged Pd^{2+} ions that successively adsorbed on the negatively charged hexacyanoferrate (HCF), then deposited as PdHCF particles on the synthesized GO surface.

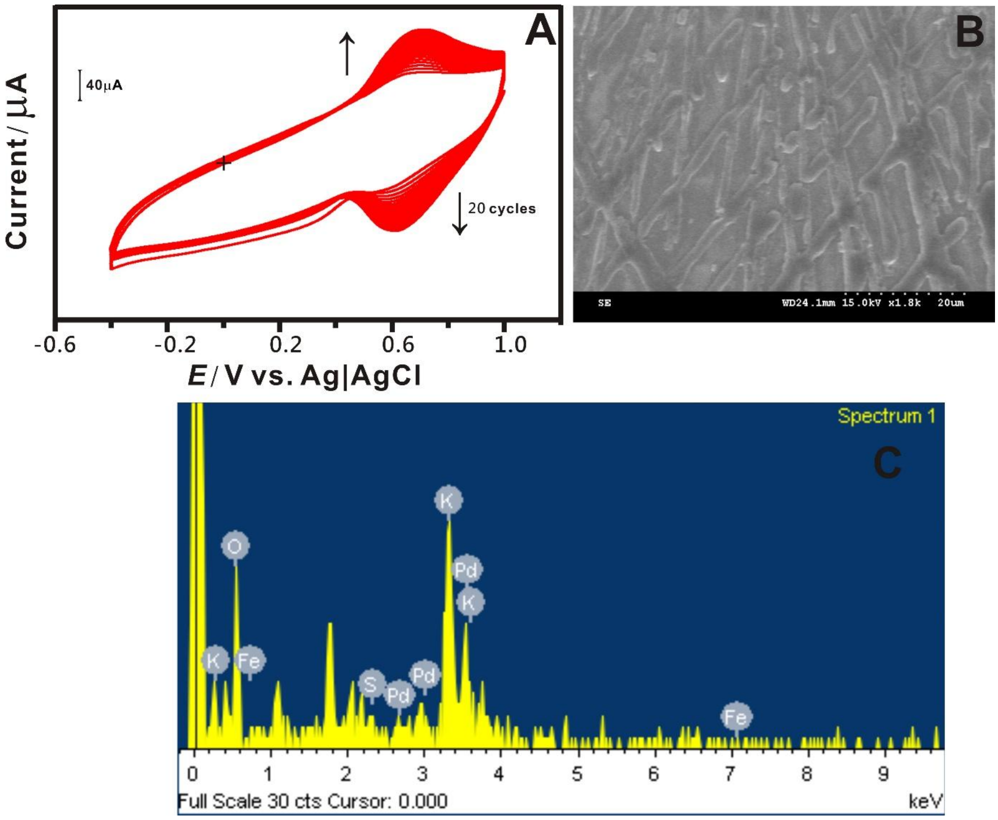

Figure 1. A) The CV of electrodeposition of PdHCF on GO/GCE at scan rate of 50 mV/s (electrolyte 0.1 M H_2SO_4). B) SEM image of PdHCF/GO C) EDX spectra of PdHCF.

The stick like structures of PdHCF enhance the anchoring strongly on GO surface. Figure 1B displays the SEM image of PdHCF on GO surface. It can be seen that stick like structure of PdHCF decorated on GO surface, which is due to the functional groups of GO interact with PdHCF particle. The result validates the PdHCF particles are electrodeposited on GO surface uniformly. Energy Dispersive X-ray (EDX) analysis of PDHCF was shown in Fig. 1C. It can be seen that all corresponding elements of PdHCF (Pd, K, Fe) shows the peak in the EDX spectrum indicates PdHCF deposited on electrode surface.

3.2 Different scan rate and pH studies

The PdHCF/GO/GCE modified GCE was investigated at different scan rate in deoxygenated PBS of pH 7.

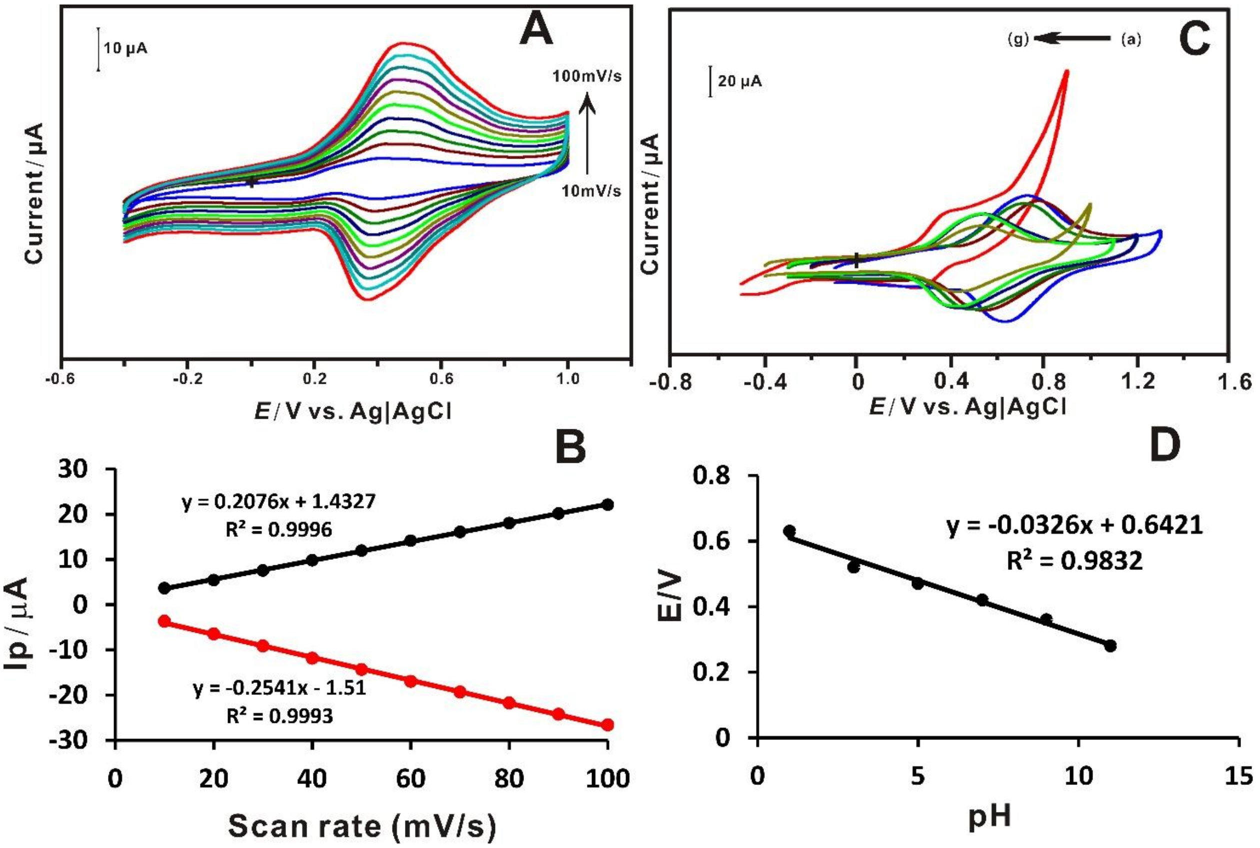

Figure 2. A) CV of PdHCF/GO/GCE in 0.05 M PBS (pH 7) at different scan rate (10 to 100 mV/s). B) Linear plot of scan rate versus current. C) CV of PdHCF/GO modified GCE on the various pH solution (a to g indicates pH 1 to 13) at scan rate of 50 mV/s. D) Linear plot of pH vs potential.

The CV responses of different scan rates are shown in Fig. 2, it can be seen that the both anodic (I_{pa}) and cathodic (I_{pc}) peak currents increased linearly with increasing the scan rates from 10 to 100 mV/s. At the scan rate of 100 mV/s, the mean peak potential was found as 420 mV. The redox peak potential separation was 90 mV for the higher scan rate. Since, the low peak separation (20 mV) at scan rate 10 mV/s and I_{pa}, I_{pc} ratio become equal to unity of surface type behavior appeared at modified electrode. The inset of Fig. 2 linear calibration plot (scan rate versus current) indicates that the modified GCE has diffusion controlled electron transfer process. According to earlier report by Razmi and Azadbakht, the redox peak is due to hexacyanoferrate single electron process in the film [28]. It was confirmed by different pH solution studies. The Fig. 2C shows the CV of GO/PdHCF modified GCE at various pH solution (1 to 11). Well defined redox peaks were observed for the wide pH range, and the redox couples are reproducible when the modified GCE was transferred from one pH solution to the other. The plot of pH versus peak potential was displayed in Fig. 2D. The slope value of -32 mV/pH was found from the plot. This value is equal to Nernst theoretical value of one electron transfer process, which was corresponding to the hexacyanoferrate single electron process in the film. However, there was no considerable decrease in the peak currents, which validates the good stability of the fabricated film.

3.3 Voltammetric determination of NIC

The PdHCF/GO composite modified GCE could be directly employed for the voltammetic detection of NIC. Relative to the bare GCE (Fig. 3A), PdHCF/GO composite modified GCE shows well defined obvious electrocatalytic peaks for the detection of NIC (peak a). At the same, only GO modification GCE , which did not show any obvious oxidation peak compared to PdHCF/GO composite modified GCE (peak a).

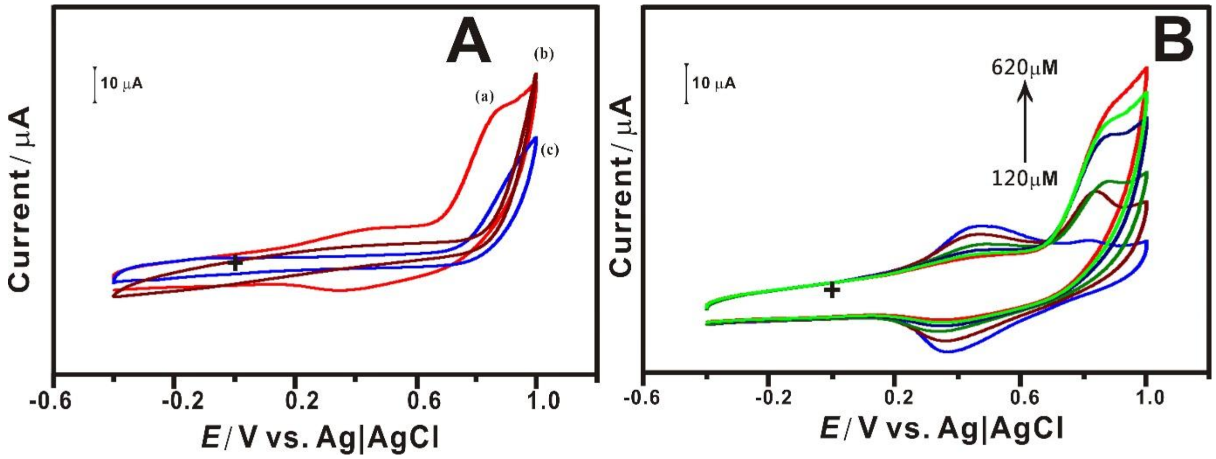

Figure 3. A) CV of PdHCF/GO modified GCE in PBS (pH 7) containing 620 μM of NIC at scan rate of 50 mV/s. B) CV of PdHCF/GO modified GCE in PBS containing various concentration of NIC.

It is high rate, seeing that fabricated GCE has exhibited NIC oxidation peak potential roughly 100 mV less potential than unmodified GCE (peak c). Finally, this CV results clearly depicts the capability of the proposed film for the detection of NIC. This arise due to the presence of PdHCF particles which acts a electroactive centers for the detection detection of NIC. In addition, the combination of GO as another layer on the surface clearly supports the surface enhancement and as well as detection of NIC.

Fig. 3B displays the CVs of PdHCF/GO modified GCE with increasing NIC concentration range from 120 to 620 μM in nitrogen saturated PBS (pH 7). It can be seen that the oxidation peak increases with addition of NIC gradually. The increase of respective oxidation peak is tailored to the NIC oxidation at the PdHCF/GO modified GCE. Thus, the direct determination of NIC via electrochemical method has been achieved by the voltammetric oxidation reaction.

3.4 Amperometric determination of NIC

The amperometric graph obtained for PdHCF/GO modified rotating ring disk electrode (RRDE) at applied potential (E_{app}) of 0.75 V was shown in Fig. 4. At regular intervals (50 s) 50 μM of NIC was injected into continuously rotated RRDE (1500 RPM) in pH 7 PBS solution. The excellent and well sharped NIC amperometric responses were observed for each and every addition of NIC. Fig.

4 shows the amperometry plot of time versus current and inset plot shows the concentration versus current. It can be seen that the linear increase of NIC oxidation current with increasing concentration of NIC.

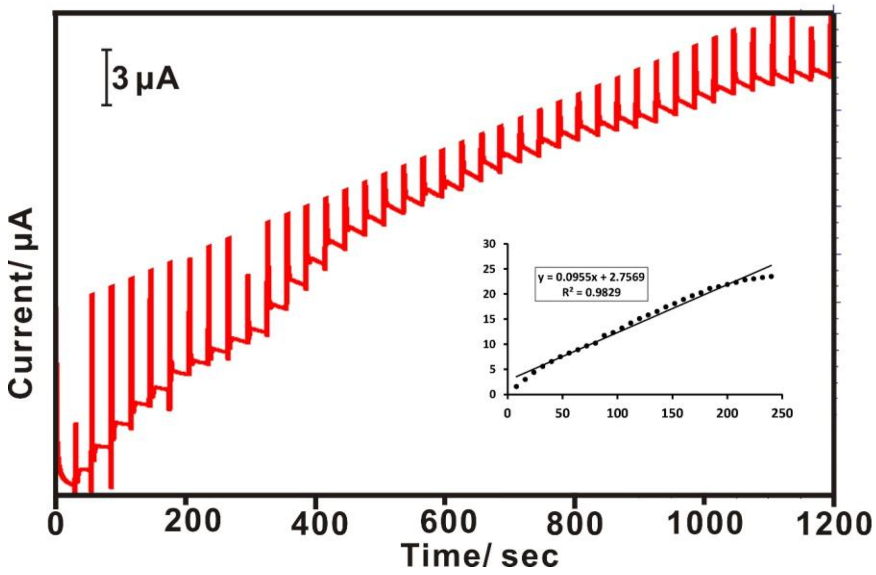

Figure 4. Amperometric response of PdHCF/GO/GCE for the sequential addition NIC in PBS solution. The inset shows the linear plot for [NIC] vs. current response.

The linear regression equation can be expressed as I = 0.0955 C (µM) + 2.756, R^2 = 0.9829. The LOD and sensitivity of the NIC sensor were calculated as 0.8 µM and 1.208 µA $\mu M^{-1} cm^{-2}$ respectively. It is specifying that related to other modified GCE, the sensitivity of NIC sensor at reported modified GCE has been calculated. Compared to MWCNT and BDD electrodes, the GO/PdHCF modified electrode shows a low overpotential for detection of NIC [41, 46]. In addition, a low limit of detection has also been obtained when compared to other reported NIC sensors, as shown in Table 1.

Table 1. Analytical comparison of proposed NIC sensor with previously reported sensors. (NA – not available)

Electrode	Sensitivity µA $\mu M^{-1} cm^{-2}$	Linear range (µM)	LOD (µM)	E_{pa} (V)	Ref
GO/PdHCF/GCE	1.2088	8 - 240	0.8	+0.75	This work
MWCNT/GCE	NA	31 - 1900	9.3	-1.4	41
NC/GCE	NA	10 - 50	5	+0.72	42
TiO_2/PEDOT/GCE	NA	0 - 5000	4.9	-	43
P(AHNSA)/GCE	NA	1 - 200	0.86	+0.86	44
CNC/SPE	NA	20 - 130	2	+0.75	45
PGE	NA	7.6 – 107.5	2	+0.84	14
AP/BDDE	NA	5 - 500	3.1	+1.30	12
BDDE	NA	0.5 – 202.5	0.3	+1.35	46

4. CONCLUSION

In conclusion, a novel composite was developed using PdHCF and GO modified GCE by electrochemical method. The fabricated composite modified GCE showed an excellent electro catalytic activity towards NIC. The CV and amperometric techniques were used for the determination of NIC at PdHCF/GO modified GCE. The fabricated film has long term stability with low overpotential and LOD. Therefore, the composite electrode can be used for the voltammetric determination of NIC.

ACKNOWLEDGEMENTS
This work was supported by ministry of science and technology. Taiwan (ROC)

References

1. C. Voelckel, T. Krugel, K. Gase, N. Heidrich, N.M. Van Dam, R. Winz, I.T. Baldwin, *Chemoecology*, 11 (2001) 121–126.
2. I. Yamamoto, J.E. Casida, Nicotinoid insecticides and the nicotinic acetylcholine receptors, Springer, Japan 1999.
3. N.L. Benowitz, Nicotine Effects and Addiction, Chapter 4, 217–244.
4. J. Banerjee, H.A.N. Al-Wadei, H.M. Schuller, *Eur. J. Cancer*, 49 (2013) 1152–1158.
5. C.C. Yu, Y.C. Chang, *Appl. Pharmacol*, 266, (2013) 459–469.
6. J. P Pierce, S. E. Cummins, M. M. White, , A. Humphrey, K. Messer, *Annual Review of Public Health*, 33 (2012) 341–356.
7. J. Jung, J. Choo, D. J. Kim, and S. Lee, Bull. *Korean Chem. Soc.* 27 (2006) **27**, 2 277.
8. T. Abdallah, S. Negm and H. Talaat, *Egypt. J. Sol.*, 25 (2002) 2.
9. J. E. Jablonski, J.E. Schilesser, and P. Mariappagoudar, *J. Agric. Food Chem.* 54 (2006) 7460-7465.
10. A.M. Massadeh, A.A. Gharaibeh, and K.W. Omari, J. Chromatogra. *Science*, 47 (2009) 170-177.
11. S.B. Stanfill, L.T. Jia, D.L. Ashley, C.H. Watson, *Journal of Chromatographic Science*, 47 (2009) 902–909.
12. H.B. Suffredini, M.C. Santos, D. De Souza, L. Codognoto, P. Homem-de-Mello, K.M. Honório, A. B. F. da Silva, S.A.S. Machado, and L.A. Avaca, *Anal. Lett.*, 38 (2005) 1587-1599.
13. L. Svorc, D.M. Stankovic, and K. Kalcher, *Diamond & Related Materials*, 42 (2014) 1–7.
14. A. Levent, Y. Yardim, Z. Senturk, *Electrochim. Acta*, 55 (2009) 190–195.
15. H.Kassa, A. Geto and S. Admassie, *Bull. Chem. Soc. Ethiop.* 27 (2013) 321-328.
16. N. R. de Tacconi, K. Rajeshwar, R.O. Lezna, *Chem. Mater.* 15 (2003) 3046-3062.
17. V.D. Neff, *J. Electrochem. Soc.*,125 (1978) 866-867.
18. C.D. Wessels, R.A. Huggins, Y. Cui, *Nature comm.*, 2 (2011) 550.
19. C. D. Wessells, S. V. Peddada, R. A. Huggins, Y. Cui, *Nano Lett.*, 11 (2011) 5421–5425.
20. M. Takachi, T. Matsuda, Y. Moritomo, *Applied Physics Express*, 6 (2013) 025802.
21. J. Chen, K. Huang , S. Liu, *Electrochem. Comm.*, 10 (2008) 1851–1855.
22. I.A. Rutkowska, A. Andrearczyk, S. Zoladek, M. Goral, K. Darowicki, P. J. Kulesza, *J Solid State Electrochem.*, 15 (2011) 2545–2552.
23. O. Sharma, M. K. Sharma, *Int. J. Chem Tech Res.*, 5 (2013) 1615–1622.
24. Y. Liu, L. Xu, Sensors 7 (2007), 2446-2457.
25. X. Wang, Y. Zhang, C. E. Banks, Q. Chenc, X. Ji, *Colloids and Surfaces B: Biointerface.*, 78 (2010) 363–366.
26. M. Rajkumar, B. Devadas, S.M. Chen, *Electrochim. Acta*,105 (2013) 439–446.
27. S.Q. Liu, Y. Chen, and H.Y. Chen, *Electroanalysis*, 14 (2002) 2.

28. H. Razmi, A. Azadbakht, *Electrochim. Acta*, 50 (2005) 2193–2201.
29. D. Ivekovic , S. Milardovic , B.S. Grabaric, *Biosens. Bioelectron.*, 20 (2004) 872–878.
30. D.l R. Dreyer, S. Park, C.W. Bielawski, R.S. Ruoff, *Chem. Soc. Rev.*, 39 (2010) 228–240.
31. D. Han Zhao, S. Palanisamy, S.M. Chen, *Int. J. Electrochem. Sci.*, 10 (2015) 10038 – 10044.
32. S. Palanisamy, H.F. Lee, S.M. Chen, B. Thirumalraj, *RSC Adv.*, 5 (2015) 105567–105573.
33. B. Thirumalraj, S. Palanisamy, S.M. Chen, C.Y. Yang, P. Periakaruppan, B.S. Lou, *RSC Adv.*, 5 (2015) 77651–77657.
34. B. Thirumalraj, S. Palanisamy, S.M. Chen, B.S. Lou, *J. Colloid Interface Sci.*, 462 (2016) 375–381.
35. C. Karuppiah, S. Palanisamy, S.M. Chen, V. Veeramani, P. Periakaruppan, *Sens. Actuators, B* 196 (2014) 450–456.
36. J. Li, J. Liu, G. Tan, J. Jiang, S. Peng, M. Deng, D. Qian, Y. Feng , Y. Liu, *Biosens. Bioelectron.*, 54 (2014) 468–475.
37. B. Devadas, M. Rajkumar, S.M. Chen, R. Saraswathi, *Int. J. Electrochem. Sci.*, 7 (2012), 3339–3349.
38. K. Subramani, D. Jeyakumar and M. Sathish, *Phys. Chem. Chem. Phys.*, 16 (2014) 4952.
39. N. Sattarahmady, H. Helid, S.E. Moradie, *Sensors and Actuators B.*, 77 (2013) 1098– 1106.
40. P.J. Kulesza , M.A. Malik, R. Schmidt , A. Smolinska, K. Miecznikowski , S. Zamponi, A. Czerwinski, M. Berrettoni , R. Marassi, *J. Electroanal. Chem.*, 487 (2000) 57–65.
41. H. Xiong, Y. Zhao, P. Liu, X. Zhang, S. Wang, *Microchim. Acta*, 168 (2010) 31–36.
42. T.W.B. Lo, L. Aldous, R.G. Compton, *Sens. Actuators B.*, 162 (2012) 361–368.
43. C.T. Wu, P.Y. Chen, J.G. Chen, V. Suryanarayanan, K.C. Ho, *Anal. Chim. Acta*, 633 (2009) 119–126.
44. A. Geto, M. Amare, M. Tessema, S. Admassie, *Electroanalysis*, 24 (2012) 659–665.
45. L. Highton, R.O. Kadara, N. Jenkinson, B.L. Riehl, C.E. Banks, *Electroanalysis*, 21 (2009) 2387–2389.
46. L. Svorc, D.M. Stankovic, K. Kalcher, *Diamond & Related Materials*. 42 (2014) 1–7.